



SEISMIC EVALUATION OF REINFORCED CONCRETE BRIDGES USING CAPACITY-BASED INELASTIC DISPLACEMENT SPECTRA

P. H. Wang⁽¹⁾, K. C. Chang⁽²⁾, D. C. Dzeng⁽³⁾, W. C. Cheng⁽⁴⁾, T. K. Lin⁽⁵⁾, H. H. Hung⁽⁶⁾,

⁽¹⁾ Assistant Technologist, National Center for Research on Earthquake Engineering, Taipei, Taiwan, phwang@ncree.narl.org.tw

⁽²⁾ Professor, Department of Civil Engineering, National Taiwan University, Taipei, Taiwan, ciekuo@ntu.edu.tw

⁽³⁾ Assistant Vice President, CECI Engineering Consultants, Inc., Taipei, Taiwan, dcdzeng@ceci.com.tw

⁽⁴⁾ Graduate Student, Department of Civil Engineering, National Taiwan University, Taipei, Taiwan, s971337@gmail.com

⁽⁵⁾ Professor, Department of Civil Engineering, National Chiao Tung University, Hsinchu, Taiwan, tklin@nctu.edu.tw

⁽⁶⁾ Research Fellow, National Center for Research on Earthquake Engineering, Taipei, Taiwan, hhung@ncree.narl.org.tw

Abstract

Capacity-based inelastic displacement spectra that comprise an inelastic displacement ratio (C_R) spectrum and the corresponding damage index (DI) spectrum were developed for far-field and near-fault ground motions to aid seismic design and evaluation of reinforced concrete (RC) bridges. It was demonstrated that the Park and Ang's damage index can be a good indicator for predicting the onset of strength deterioration and assessing the actual visible damage condition of column regardless of its loading history, providing a better insight into the seismic performance of bridges. To investigate the accuracy and applicability of the spectra, an example bridge was constructed and analyzed by using various structural analysis programs, such as SAP2000, OpenSees, and a smooth hysteresis model (SHM). Nonlinear time history analyses of the bridge were conducted for far-field and near-fault ground motions. It was found that the differences of the analytical results between various models was closely related to the structural periods of bridge as well as the considered ground motion characteristics. Moreover, the SAP2000 and OpenSees models could underestimate the seismic responses of bridge especially for long period bridges, and the computed errors could reach 16.8% and 13.2%, respectively, as compared to the SHM model. Besides, seismic evaluations of the example bridge by using the capacity-based inelastic displacement spectra and the response modification factor (R_d) provided by AASHTO's Guide Specification for LRFD Seismic Bridge Design were also conducted in this study. When compared to nonlinear time history analysis results, the capacity-based inelastic displacement spectra can satisfactorily predict not only the inelastic displacement but also the corresponding damage state of bridge both for far-field and near-fault ground motions. In contrast, the AASHTO's R_d formula can receive similar inelastic displacement estimations to the C_R formula of the capacity-based spectra for far-field ground motions. However, it cannot reflect the response amplification effects caused by the frequency-content characteristics of near-fault ground motions, and therefore could significantly underestimate the inelastic responses of bridge.

Keywords: Reinforced concrete; bridge; inelastic displacement; damage index; near-fault



1. Introduction

Seismic evaluation methods of structural system can be broadly classified into two categories, namely nonlinear time history analysis and simplified methods, according to the level of analytical precision. Nonlinear time history analysis can receive the most comprehensive and exact seismic assessment results. However, a large number of efforts in terms of sophisticated modeling skills and computation costs are needed. On the other hand, simplified methods, such as capacity spectrum method (ATC-40) and displacement coefficient method (FEMA 273), were proposed to facilitate the analytical work. In general, the simplified method methods can reach approximate evaluation results, and mainly apply to structural systems with regular configurations. Capacity spectrum method was featured by its graphical implementation of intersection between capacity and demand spectra. However, it was revealed by Krawinkler (1995) that there is no physical principle to justify the use of highly damped elastic spectra for determining the seismic demand of structure. Thereafter, the method was improved by making use of inelastic response spectrum to replace the highly damped elastic spectrum, and the improved method was then practically equivalent to the displacement coefficient method. Recently, it can be observed from current seismic design and evaluation of bridges that the displacement coefficient method has become a main trend.

Capacity-based inelastic displacement spectra that comprised an inelastic displacement ratio (C_R) spectrum and the corresponding damage index (DI) spectrum for RC bridge columns (Wang et al., 2019) was constructed based on the displacement coefficient method. It was demonstrated that the Park and Ang's damage index can be a good indicator for predicting the onset of strength deterioration and assessing the actual visible damage condition of column regardless of its loading history, providing a better insight into the seismic performance of bridges. Therefore, it was considered that inelastic displacement associated with the corresponding damage index can be more sufficient and comprehensive to tell the seismic performance of structures as compared to the displacement assessment only. In order to investigate the accuracy and applicability of the spectra, an example bridge was constructed and analyzed by using various structural analysis programs, such as SAP2000, OpenSees, and a smooth hysteresis model (Wang et al., 2017). Nonlinear time history analyses of the bridge were conducted for far-field and near-fault ground motions, and used to evaluate the capacity-based inelastic displacement spectra. Besides, the displacement modification factor R_d provided by AASHTO's Guide Specification for LRFD Seismic Bridge Design (2011), was also examined in this study.

2. Capacity-Based Inelastic Displacement Spectra

Capacity-based inelastic displacement spectra for RC bridge columns were proposed by Wang et al. (2019). The spectra were composed of an inelastic displacement ratio (C_R) spectrum and the corresponding damage index (DI) spectrum, forming a dual spectrum. The inelastic displacement ratio (C_R) was based on systems with a constant lateral strength and defined as

$$C_R = \frac{\Delta_{inelastic}}{\Delta_{elastic}} \quad (1)$$

where $\Delta_{inelastic}$ is the maximum inelastic displacement of a SDOF system with a 5% viscous damping ratio and a lateral yield strength F_y while $\Delta_{elastic}$ is the maximum elastic displacement of the corresponding elastic system having the same T_n and subjected to the same earthquake ground motion. The lateral strength of the system is described by a relative strength ratio R (or strength reduction factor), which is defined as

$$R = \frac{mS_a}{F_y} \quad (2)$$

where m is the mass of the system, and S_a is the elastic spectral acceleration.

The damage index was proposed by Park and Ang (1985) and defined as

$$DI = \frac{\delta_m}{\delta_u} + \lambda \frac{\int dE}{F_y \delta_u} \quad (3)$$



where δ_m is the maximum displacement of column; δ_u is the ultimate displacement capacity of column under monotonic loading; $\int dE$ is the accumulated hysteretic energy dissipation; and λ is a parameter to correlate hysteretic energy dissipation to damage, which can be calculated by setting DI equal to one at the ultimate state of column when the strength of column drops to 80% of its peak value.

Nonlinear time history analyses of SDOF systems were conducted to construct the spectra by using a new smooth hysteretic model (Wang et al. 2017), that can realistically simulate the degrading hysteresis behaviors of RC columns and accurately capture its strength deterioration via the Park and Ang's damage index (1985) regardless of its loading history (Fig. 1). Furthermore, it was also demonstrated that the damage index can be a good indicator for assessing the actual visible damage condition of column, ingeniously bridging the analytical results and actual damage pictures as illustrated in Fig. 2. Therefore, the inelastic displacement ratio C_R associated with the damage index DI can provide a better insight into the seismic performance of RC bridges.

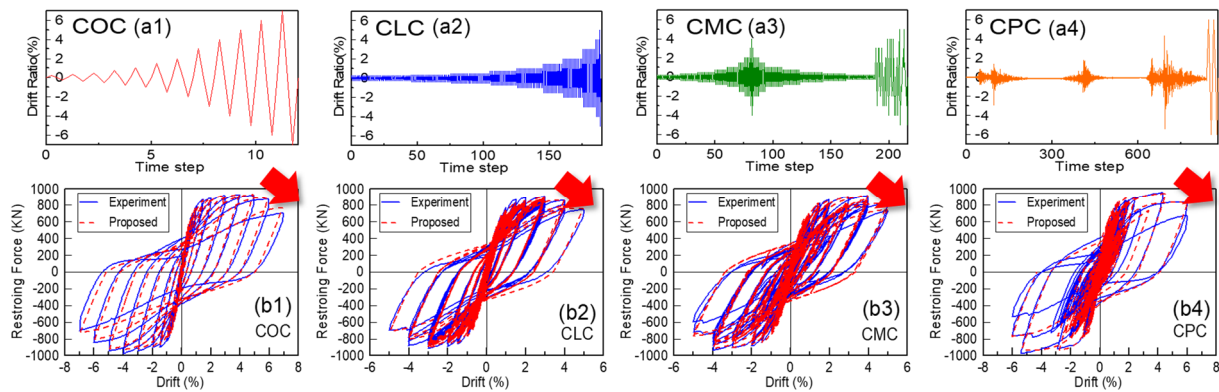


Fig. 1 – (a) Loading history; (b) Comparison between experimental and analytical hysteresis loops

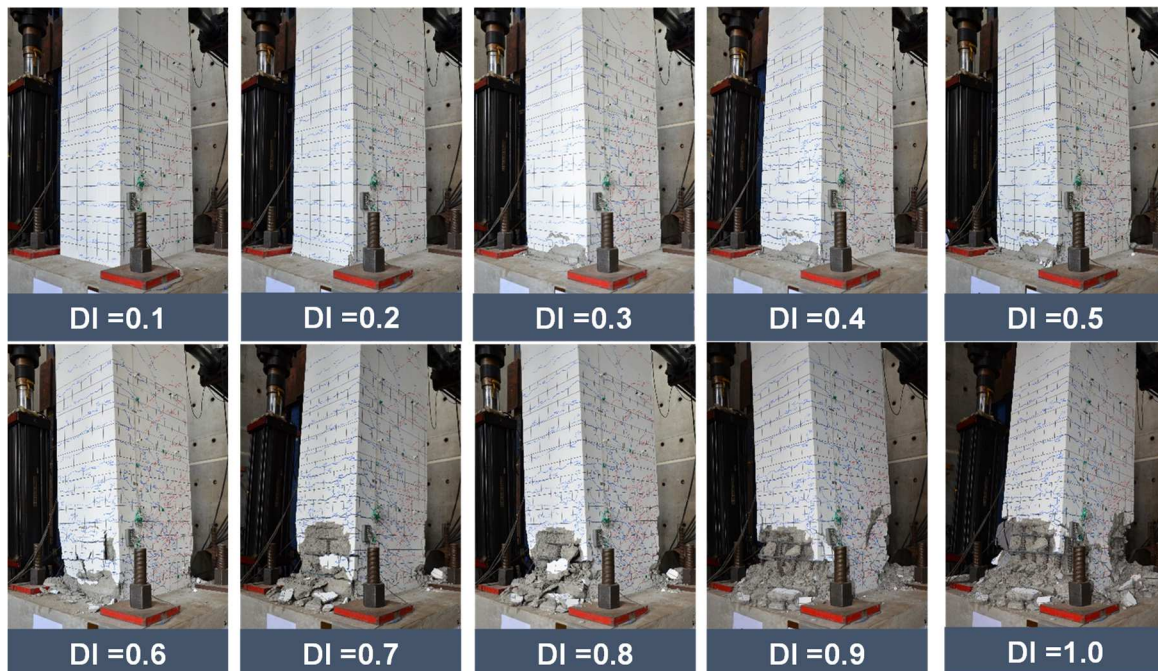


Fig. 2 – Correlations between damage index and actual damage condition



The capacity-based inelastic displacement spectra were constructed for far-field and near-fault ground motions, respectively. For far-field ground motions, two site classes, namely site classes C (denoted as FFC) and D (denoted as FFD) in accordance with the NEHRP classification (2004), were considered. On the other hand, the near-fault ground motions with the pulse-like characteristics were classified into three pulse period (T_p) ranges based on the magnitude of T_p . The three T_p ranges, denoted as NF1, NF2, and NF3, have period ranges of 0.5 s - 2.5 s (i.e., including 0.5 s but excluding 2.5 s), 2.5 s - 5.5 s, and 5.5 s - 10.5 s, respectively. The pulse period of each near-fault record was extracted by Baker (2007) using wavelet analysis. Fig. 3 illustrated the capacity-based inelastic displacement spectra for specific design parameters of RC columns under FFC. It can be seen in the Figure that each spectral curve associated with a given relative strength ratio R possesses a period limit. If the period of vibration is shorter than this limit there will be no spectral ordinate or no result. In other words, for a given relative strength ratio R a system with period of vibration shorter than this period limit would fail or collapse under the considered earthquakes. The capability to tell the performance state of a system discriminates the capacity-based spectra from the classical inelastic response spectra that only provide seismic demand assessments. Detailed calculated spectra and spectral formula can be found in Wang et al. (2019).

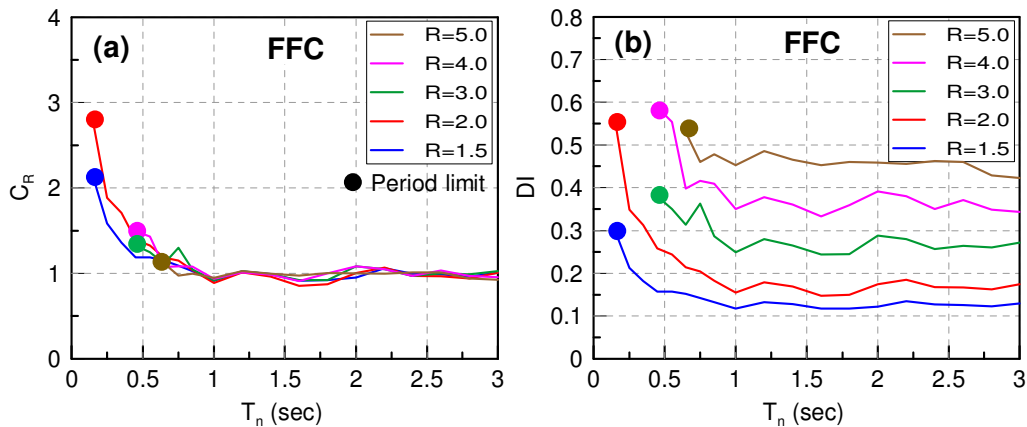


Fig. 3 – Illustration of capacity-based inelastic displacement spectra: (a) inelastic displacement ratio spectrum; (b) corresponding damage index spectrum

3. Example Bridge and Ground Motion Records

3.1 Example bridge

To realize the applicability of the capacity-based inelastic displacement spectra to the seismic evaluation of RC bridges, an example bridge was constructed and analyzed by using various structural analysis programs, such as SAP2000, OpenSees, and the smooth hysteresis model (Wang et al., 2017). Fig. 4 shows the configuration of the example bridge, which is a three-span continuous prestressed reinforced concrete box girder bridge with balanced stiffness and frame geometry. The columns are fixed at the bottom where the soil-structure interaction is not considered in this study. On the other hand, the bridge deck is supported by two hinge bearings at each of the middle two bents, and by two roller bearings at each of the end bents along the longitudinal direction of bridge. However, in the transverse direction of bridge, the roller bearings at the end bents are locked to prevent lateral movement. The bridge is assumed to be located in Nantou county of central Taiwan and near the Chelungpu fault. According to the current seismic bridge design code (MOTC, 2019), the peak ground accelerations (PGA) of the bridge under design and maximum credible earthquakes 0.36 g and 0.45 g, respectively. Furthermore, the force reduction factors of the bridge in the longitudinal and transverse directions are calculated to be about 3.14 and 1.50, respectively, in accordance with the design spectrum of maximum credible earthquake. Detailed column reinforcements can be found in Fig. 4.

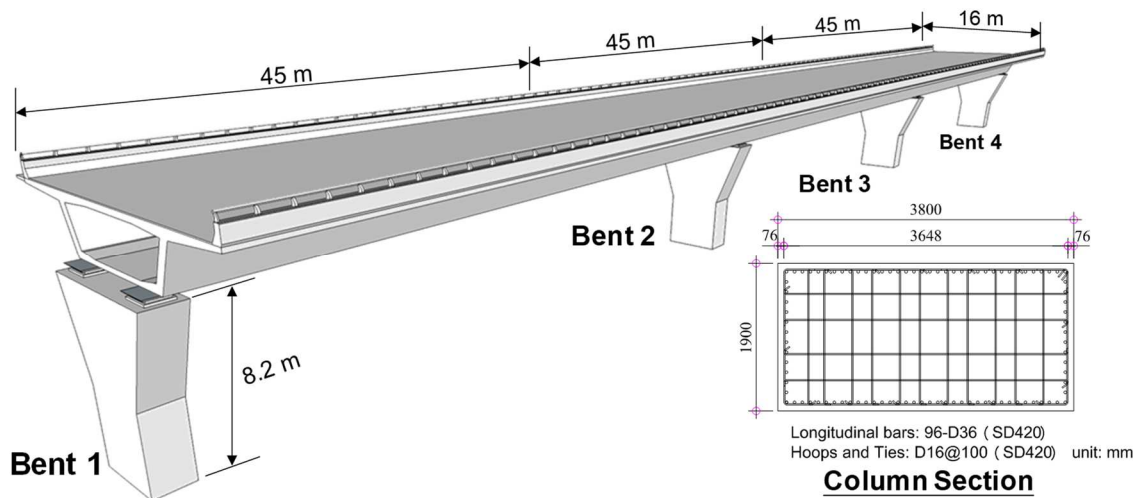


Fig. 4 – Configuration of example bridge

Three analytical models constructed using SAP2000, OpenSees, and a new smooth hysteretic model (SHM), respectively, were used to analyze the seismic responses of the example bridge. In the three analytical models, the SAP2000 and OpenSees models are 3D whole bridge models while the new smooth hysteretic model is an equivalent SDOF model. In the 3D bridge models, the effect of adjacent frames on the transverse seismic responses of the bridge was considered by adding the masses contributed from adjacent frames to the end bents of the bridge on the assumption that the adjacent frames had similar configurations to the example bridge. Fig. 5 shows the fundamental modes of the example bridge computed from the SAP2000 model in the longitudinal and transverse directions, whose fundamental periods of vibration (T_n) are 0.82 s and 0.46 s, respectively. Moreover, the modal participating mass ratios of the fundamental modes are 0.89 and 0.94 in the longitudinal and transverse directions, respectively.

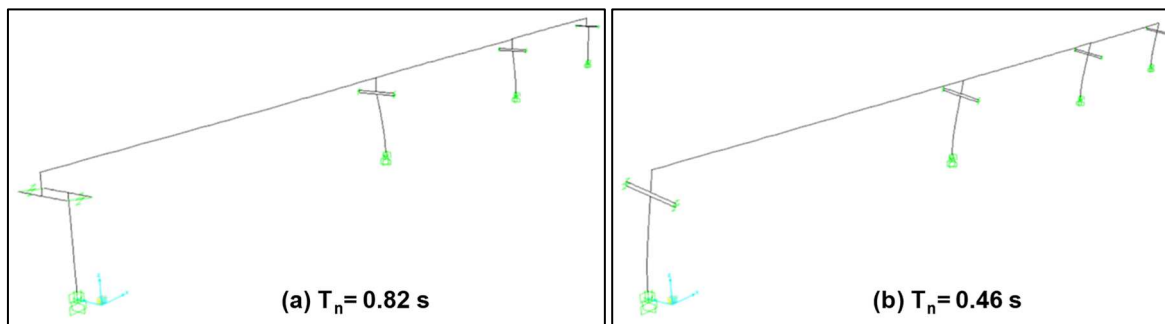


Fig. 5 – Fundamental modes of example bridge: (a) longitudinal direction; (b) transverse direction

Simulating the nonlinear behavior of bridge column is the most important and critical issue in constructing a bridge model since it would dominate the seismic responses of a bridge. In the SAP2000 bridge model, nonlinear link with Takeda hysteretic behavior was used in the probable plastic hinge region of column. It should be noticed that the Takeda model embedded in SAP2000 did not consider stiffness degradation, which was practically equivalent to the Modified Clough model (1976). In the OpenSees bridge model, the distributed plasticity approach was used to simulate the nonlinear behavior of bridge column, where the fiber section was defined at the integration points of force-based beam-column element. Furthermore, the fiber section was divided into small pieces of material fibers to define the constitutive materials of column that included the unconfined cover concrete, confined core concrete, and longitudinal steel. And the uniaxial material models, namely the concrete02 and steel02, were utilized to simulate the hysteretic behaviors of concrete and steel materials, respectively. Finally, the constructed OpenSees model was calibrated so that it could reach comparable pushover behavior to that of the SAP2000 bridge model.



The example bridge was very regular with balanced mass, stiffness, and geometry such that it could approximately respond to an earthquake in its fundamental mode of vibration. Two equivalent SDOF bridge models were established to approximate the seismic behaviors of the example bridge in the longitudinal and transverse directions, respectively. The SDOF bridge models were characterized by the new smooth hysteretic model mentioned above, whose model parameters were identified from the experimental results of RC columns having similar design parameters with the example bridge columns. Besides, the initial stiffness, the maximum lateral strength, and the equivalent mass of the SDOF model were calibrated from the SAP2000 bridge model.

3.2 Ground motion records

To obtain comparable analytical results between the nonlinear time history analysis of the example bridge and the capacity-based inelastic displacement spectra, the ground motion records were normalized based on the constant strength (R) assumption used for computing the capacity-based spectra. On the other hand, it was revealed in Wang et al. (2019) that the near-fault ground motions would result in greater nonlinear responses and damages than the far-field ground motions under the basis of the same R . Therefore, the far-field and near-fault ground motions were normalized to have relative strength ratios (R) equal to 3.0 and 5.0, respectively, at the fundamental vibration periods of the example bridge in the considered analysis direction. The selection of large R was intended to compare the ability to simulate significant nonlinear responses of bridge between various analytical models. Fig. 6 illustrates the methodology to normalize the ground motions, where S_{ay} is the maximum spectral acceleration obtained from the pushover curve of the example bridge in the considered direction when converted into Acceleration-Displacement Response Spectrum (ADRS) format. For far-field ground motions, the S_{ay} was multiplied by $R = 5.0$ to obtain the normalized elastic response spectral ordinate, which was then divided by spectral ordinate of each ground motion record at the considered fundamental vibration period of bridge to obtain the corresponding coefficient of magnification (C_{mag}). For near-fault ground motions, the C_{mag} of each record can be calculated by using $R = 3.0$. Table 1 lists the coefficients of magnification for far-field (FFC & FFD) and near-fault (NF1~NF3) ground motions, where each category contains 15 records. The far-field records resulted from 10 different earthquake events with moment magnitude (M_w) ranging from 6.0 to 7.6. And the near-fault records with the pulse-like characteristics were obtained from 13 different earthquake events with M_w ranging from 5.7 to 7.6. Detailed informations about the selected ground motion records can be found in Wang et al. (2019).

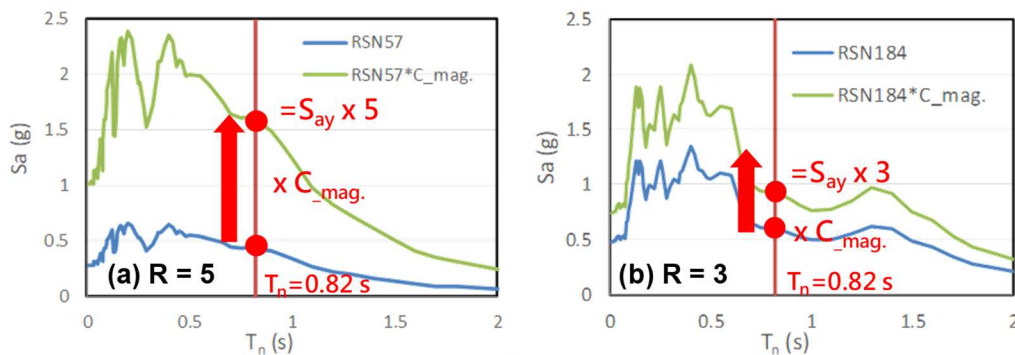


Fig. 6 – Illustrations of normalizing the ground motion records for (a) far-field (FFC & FFD); and (b) near-fault (NF1~NF3) ground motions

Table 1 – Coefficients of magnification for ground motion normalization

No.	RSN	C_{mag}													
		Long.	Trans.												
FFC01	57	3.53	6.54	FFD01	66	40.60	52.22	NF101	77	0.90	1.22	NF201	161	3.07	4.70
FFC02	164	3.73	10.63	FFD02	93	19.39	28.57	NF102	150	1.21	3.22	NF202	179	2.11	3.73
FFC03	265	2.96	3.69	FFD03	169	3.51	6.30	NF103	159	2.76	4.41	NF203	181	1.59	3.39
												NF301	184	1.55	2.04
												NF302	803	1.36	4.96
												NF303	838	4.04	12.64



FFC04	610	18.16	18.31	FFD04	316	4.46	6.00	NF104	568	0.93	2.02	NF204	767	2.18	4.16	NF304	900	2.18	5.12
FFC05	771	4.45	8.84	FFD05	652	8.87	12.67	NF105	764	2.53	2.95	NF205	802	2.02	4.72	NF305	1148	5.38	13.81
FFC06	787	4.56	5.01	FFD06	653	42.49	26.33	NF106	766	1.85	2.92	NF206	828	0.67	1.64	NF306	1161	2.79	4.82
FFC07	875	37.55	55.64	FFD07	777	2.07	5.54	NF107	1004	0.67	1.07	NF207	879	1.54	3.35	NF307	1491	2.87	5.38
FFC08	1019	7.17	16.46	FFD08	790	3.68	19.52	NF108	1044	0.67	1.48	NF208	982	0.61	1.76	NF308	1498	2.63	4.93
FFC09	1072	12.62	18.31	FFD09	800	11.43	18.60	NF109	1050	2.48	1.91	NF209	983	0.86	1.09	NF309	1501	1.83	4.88
FFC10	1073	16.84	13.26	FFD10	836	16.20	23.97	NF110	1086	0.88	0.99	NF210	1045	0.99	3.14	NF310	1503	1.00	3.24
FFC11	1172	33.28	49.93	FFD11	965	24.56	16.22	NF111	1106	0.48	0.96	NF211	1084	0.56	1.64	NF311	1515	2.14	3.86
FFC12	1295	6.74	23.03	FFD12	1094	19.49	19.01	NF112	1119	0.79	1.29	NF212	1114	1.45	4.06	NF312	1519	6.15	5.96
FFC13	1315	36.25	37.29	FFD13	1237	8.10	17.80	NF113	1120	0.61	1.55	NF213	1182	1.15	2.14	NF313	1528	2.57	4.69
FFC14	1471	7.46	12.01	FFD14	1304	5.33	7.93	NF114	1602	1.11	1.34	NF214	1510	2.68	3.27	NF314	1531	6.71	11.31
FFC15	1837	16.94	29.39	FFD15	1540	10.29	15.36	NF115	3746	1.58	2.12	NF215	3473	2.18	4.79	NF315	6975	4.38	4.30

Note: RSN is the record sequence number used in PEER ground motion database.

4. Nonlinear Time History Analysis Results

Nonlinear time history analysis of the example bridge was conducted by using three analytical models when subjected to 30 far-field and 45 near-fault ground motions listed in Table 1. Both the longitudinal and transverse directions of bridge were considered, and therefore a total of 150 cases were analyzed by each model. Fig. 7 shows the selected analytical results of the three bridge models that depict the relationship between the deck lateral displacement and base shear in the longitudinal direction of the bridge under NF3. Fig. 8 further shows the corresponding time history of deck displacement to the cases shown in Fig. 7. The red, green, and blue lines represent the analytical results from the new smooth hysteretic model (SHM), SAP2000, and OpenSees models, respectively. It should be reminded that the base shear obtained from the SAP2000 model contained the contributions from inherent damping forces while those from the OpenSees and SHM did not. By comparing the analytical results from various bridge models, major observations can be summarized as follows: (a) the OpenSees and SHM models could generate very similar and realistic hysteresis behaviors while the hysteresis shape of the SAP2000 model was too full and could not feature the stiffness degradation and pinching behavior of RC members; (b) the SAP2000 model would frequently produce apparent residual displacement at the end of an earthquake event as compared to the other two models; (c) the near-fault ground motions would cause uneven hysteresis responses more easily than the far-field ground motions, resulting in large inelastic displacements occurred in one direction of bridge; (d) in general, the SHM and SAP 2000 models would receive the maximum and the minimum inelastic displacements, respectively, among the three analytical models when subjected to the same ground motion event; (e) the SHM model can well simulate the strength deterioration of bridge in an adaptive manner to the ground motion characteristics when compared to the other models.

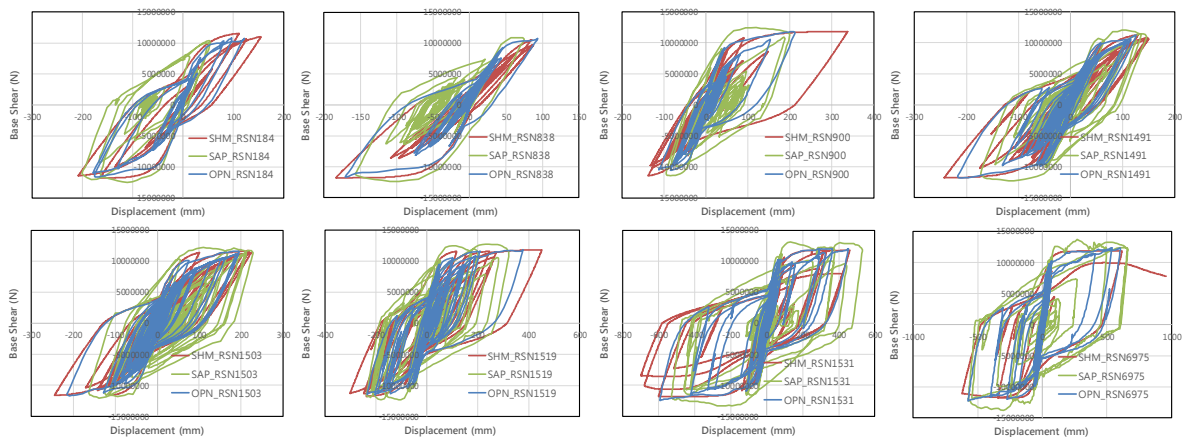


Fig. 7 – Comparison of hysteresis loops between various analytical models in the longitudinal direction of bridge under NF3

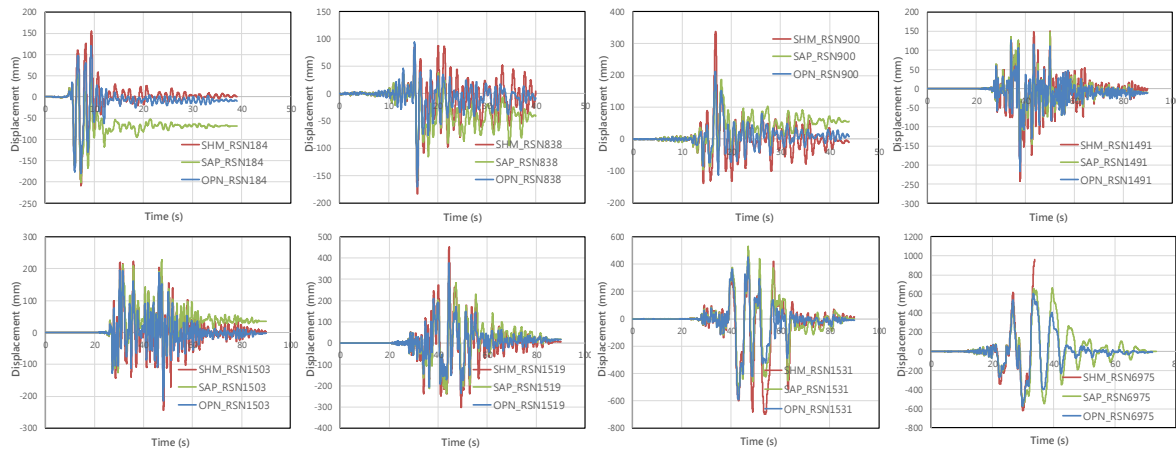


Fig. 8 – Comparison of deck displacement histories between various analytical models in the longitudinal direction of bridge under NF3

Tables 2 and 3 summarize the differences of the computed deck displacements between various analytical models when subjected to different ground motion categories in the longitudinal and transverse directions, respectively. In the comparisons, it was assumed that the SHM can satisfactorily simulate the seismic responses of the example bridge, and therefore was considered to be accurate as compared to the SAP2000 and OpenSees models. This assumption was based on the analytical results of a bridge column that was tested using pseudo-dynamic loading with three consecutive long-duration ground motions (Wang et al, 2017). Fig. 7 compares the experimental and analytical hysteresis loops of the column conducted by using SHM, Modified Clough model, and OpenSees model, where the SHM had the best precision. Considering the seismic responses of bridge was a cyclic behavior with positive and negative displacements, three displacement assessing measures, namely the maximum positive displacement (Δ_{max}), the minimum negative displacement (Δ_{min}), and the maximum absolute value of displacements ($|\Delta_i|$), were compared in Tables 2 and 3. It should be noticed that the computed error listed in the tables was the average value among the 15 records of specific ground motion category. And once the SHM showed collapse under certain ground motion record, that analytical case would be exempted from averaging the errors both for the SAP2000 and OpenSees models. The collapse status in SHM was defined such that the computed damage index was larger than one at the end of analysis, or dynamic instability occurred before the end of analysis.

According to Tables 2 and 3, important conclusions can be drawn as follows: (a) the computed errors in the longitudinal direction of bridge ($T_n = 0.82$ s) were apparently greater than those in the transverse direction of bridge ($T_n = 0.46$ s), which was inferred to be closely related to the magnitude of the vibration period of bridge; (b) in general, the computed errors under near-fault ground motions were larger than those under far-field ground motions; (c) the SAP2000 model would frequently produce biased hysteresis behaviors, resulting in larger variance of errors between Δ_{max} and Δ_{min} , as compared to the OpenSees model; (d) the OpenSees model as more accurate than the SAP2000 model for all ground motion categories and analytical directions of bridge considered in this study; (e) by averaging the errors of Δ_{max} , Δ_{min} , and $|\Delta_i|$, the OpenSees model in the longitudinal direction of bridge would produce average errors of -6.9% and -13.2% under FFC and NF3, respectively, while the corresponding values for SAP2000 model were -9.7% and -16.8%; (f) in contrast, the OpenSees model in the transverse direction of bridge would produce average errors of +1.7% and +3.7% under FFC and NF3, respectively, while the corresponding values for SAP2000 model were -5.9% and -2.5%. Finally, it was suggested that the analytical resulted obtained from the OpenSees and SAP2000 models be appropriately magnified, especially for long period structures, to avoid underestimation of seismic responses and therefore lead to unconservative evaluation results.

Table 2 – Differences of analyzed longitudinal displacement of bridge as compared to SHM



Earthquake Category	OpenSees Error (%)				SAP2000 Error (%)			
	Δ_{max}	Δ_{min}	$ \Delta_i $	Avg.	Δ_{max}	Δ_{min}	$ \Delta_i $	Avg.
FFC	-6.6	-6.0	-8.0	-6.9	-2.0	-21.6	-5.5	-9.7
FFD	-10.6	-13.2	-9.3	-11.0	-27.2	-5.3	-7.2	-13.3
NF1	-13.7	-8.6	-6.7	-9.7	-24.8	-16.7	-13.5	-18.3
NF2	-9.4	-7.2	-9.6	-8.7	-10.2	-23.8	-8.4	-14.1
NF3	-16.6	-10.4	-12.6	-13.2	-18.9	-16.9	-14.7	-16.8

Table 3 – Differences of analyzed transverse displacement of bridge as compared to SHM

Earthquake Category	OpenSees Error (%)				SAP2000 Error (%)			
	Δ_{max}	Δ_{min}	$ \Delta_i $	Avg.	Δ_{max}	Δ_{min}	$ \Delta_i $	Avg.
FFC	1.9	1.7	1.5	1.7	2.9	-20.9	0.3	-5.9
FFD	1.3	-1.6	-1.1	-0.5	-11.7	-7.4	-4.1	-7.7
NF1	4.3	6.3	2.7	4.4	-5.6	-7.0	-0.3	-4.3
NF2	3.9	9.6	1.4	4.9	-5.1	-14.4	-5.8	-8.4
NF3	1.3	6.7	3.3	3.7	2.2	-7.5	-2.1	-2.5

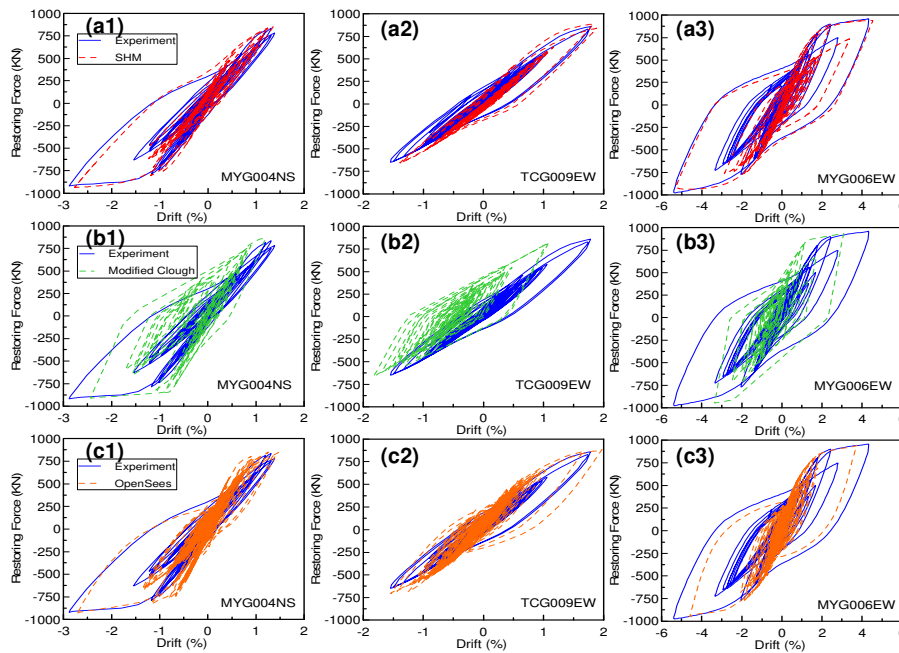


Fig. 7 – Comparisons between experimental and analytical hysteresis loops conducted by using: (a) SHM; (b) Modified Clough model; (c) OpenSees model

5. Seismic Evaluation Using Capacity-Based Inelastic Displacement Spectra

The nonlinear time history analysis results of the example bridge conducted in this study was then used to examine the accuracy and applicability of the capacity-based inelastic displacement spectra. Besides, the displacement modification factor R_d , which was equivalent to the C_R and provided by AASHTO's Guide Specification for LRFD Seismic Bridge Design (2011), was also examined in this section. The R_d formula was given as follows.



$$R_d = \begin{cases} \left(1 - \frac{1}{\mu_D}\right) \frac{T^*}{T_n} + \frac{1}{\mu_D}, & T_n < T^* \\ 1.0, & T_n \geq T^* \end{cases} \quad (4)$$

where $T^* = 1.25T_s$, and T_s is the characteristic or corner period of elastic response spectrum; μ_D is the maximum local member displacement ductility demand, and the guide specification suggests $\mu_D = 6.0$ for high seismicity region (i.e., Seismic Design Category, SDC D) in lieu of detailed analysis. It should be reminded that Eq. (4) is identical to the C_R formula of the capacity-based spectra for FFC (Wang et al., 2019), when μ_D is replaced by R . Besides, the C_R formula for FFC is also exactly identical to the factor R_d in the seismic retrofitting manual for highway structures (part 1-bridges) published by Federal Highway Administration (FHWA 2006).

Fig. 8 illustrates seismic evaluations of the example bridge using the capacity-based inelastic displacement spectra. First of all, the dual spectra (C_R and DI spectra) can be obtained by substituting the major design parameters of bridge column, such as the reinforcement ratios of longitudinal and transverse steels as well as the aspect ratio, into the spectral formulae of certain ground motion category (Wang et al., 2019). According to the fundamental period (T_n) and relative strength ratios (R) of the example bridge in the considered direction, the inelastic displacement ratio and the corresponding damage index then can be easily calculated.

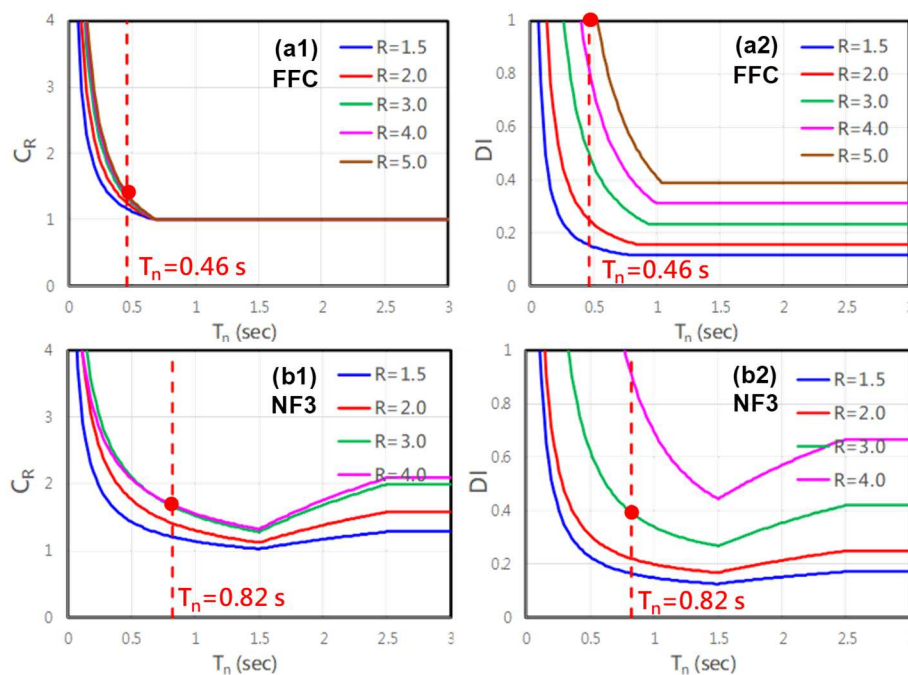


Fig. 8 – Illustration of using capacity-based inelastic spectra for seismic evaluation of example bridge in the: (a) transverse direction under FFC; (b) longitudinal direction under NF3

Table 4 lists the selected evaluation results of the longitudinal direction of example bridge under FFC and NF3. For long period region, both the capacity-based spectra (under FFC) and AASHTO's R_d formula comply with the equal-displacement rule, namely $C_R = 1.0$ and $R_d = 1.0$, which agree with the average $C_R = 0.97$ computed from the nonlinear time history analyses of the example bridge using SHM (as shown in Table 4a). Besides, the DI formula of capacity-based spectra can also predict well the average DI computed from the nonlinear time history analyses, while the AASHTO's formula could not provide information about the damage state of bridge. For near-fault ground motions, Table 4(b) also indicates that the capacity-based spectra's formulae can also receive satisfactory evaluation results when compared with the nonlinear time history analyses of bridge. However, the AASHTO's formula cannot reflect the response amplification effects caused by the frequency-



content characteristics of near-fault ground motions, and therefore the formula would significantly underestimate the inelastic responses of bridge.

Table 4 – Seismic evaluation of the longitudinal direction of example bridge under: (a) FFC; (b)NF3

(a)SHM(FFC), $T_n=0.82$ sec, $R=5.0$			(b)SHM (NF3), $T_n=0.82$ sec, $R=3.0$		
RSN	$C_R = \Delta_i / \Delta_e$	DI	RSN	$C_R = \Delta_i / \Delta_e$	DI
57	0.69	0.26	184	1.35	0.30
164	0.79	0.38	803	1.52	0.33
265	1.02	0.41	838	1.19	0.25
610	0.51	0.19	900	2.19	0.48
771	1.13	0.41	1148	1.09	0.23
787	1.31	0.54	1161	0.82	0.16
875	1.36	0.72	1491	1.57	0.37
1019	0.74	0.29	1498	1.88	0.53
1072	0.65	0.26	1501	1.10	0.26
1073	0.65	0.27	1503	1.59	0.47
1172	1.15	0.44	1515	1.04	0.24
1295	3.03	1.38	1519	2.93	0.81
1315	1.95	1.11	1528	1.79	0.38
1471	3.09	1.46	1531	–	–
1837	0.71	0.35	6975	–	–
Calculated Avg.	0.97	0.43	Calculated Avg.	1.54	0.37
Capacity-Based Spectra	1.00	0.50	Capacity-Based Spectra	1.66	0.39
AASHTO R_d Formula	1.00	–	AASHTO R_d Formula	1.00	–

Table 5 lists the selected evaluation results of the transverse direction of example bridge under FFC and NF3. For far-field ground motions (FFC), the C_R and R_d formulae can receive similar estimations of inelastic displacement ratio since the value of $R=5.0$ is very close to that of $\mu_D=6.0$ in the corresponding formulae. Moreover, the DI formula indicates that the bridge has collapsed (i.e., $DI=1.23 > 1.0$), which conservatively reflect most of the analysed cases (8 of 15) have gain severe damage ($DI > 0.7$) in the nonlinear time history analyses of bridge. For near-fault ground motions, similar tendency to that in Table 4(b) can also be observed in Table 5(b).

Table 5 – Seismic evaluation of the transverse direction of example bridge under: (a) FFC; (b)NF3

(a)SHM(FFC), $T_n=0.46$ sec, $R=5.0$			(b)SHM (NF3), $T_n=0.46$ sec, $R=3.0$		
RSN	$C_R = \Delta_i / \Delta_e$	DI	RSN	$C_R = \Delta_i / \Delta_e$	DI
57	1.11	0.55	184	1.01	0.23
164	2.39	1.52	803	–	–
265	1.14	0.51	838	2.85	0.71
610	0.68	0.32	900	3.68	0.90
771	2.12	0.87	1148	3.01	0.72
787	1.04	0.46	1161	1.61	0.36
875	1.14	0.70	1491	1.20	0.34
1019	2.01	0.89	1498	1.73	0.55
1072	1.10	0.57	1501	2.01	0.55



1073	0.56	0.24	1503	–	–
1172	1.36	0.58	1515	1.09	0.28
1295	–	–	1519	0.93	0.25
1315	1.50	0.77	1528	1.58	0.39
1471	2.98	1.40	1531	2.54	0.70
1837	1.49	0.72	6975	1.37	0.33
Calculated Avg.	1.27	0.60	Calculated Avg.	1.89	0.48
Capacity-Based Spectra	1.40	1.23	Capacity-Based Spectra	2.19	0.77
AASHTO R_d Formula	1.41	–	AASHTO R_d Formula	1.41	–

6. Conclusions

- (1). It was found from the nonlinear time history analysis of example bridge that the differences of the analytical results between various models was closely related to the structural periods of bridge as well as the considered ground motion characteristics.
- (2). SAP2000 and OpenSees models could underestimate the seismic responses of bridge especially for long period bridges, and the computed errors could reach 16.8% and 13.2%, respectively, as compared to the SHM model.
- (3). Capacity-based inelastic displacement spectra can satisfactorily predict not only the inelastic displacement but also the corresponding damage state of bridge both for far-field and near-fault ground motions.
- (4). AASHTO's R_d formula can receive similar inelastic displacement estimations to the C_R formula of the capacity-based spectra for far-field ground motions. However, it cannot reflect the response amplification effects caused by the frequency-content characteristics of near-fault ground motions, and therefore could significantly underestimate the inelastic responses of bridge.

7. References

- [1] Applied Technology Council (1996): Seismic Evaluation and Retrofit of Concrete Buildings. Report ATC 40, Redwood City, California.
- [2] Federal Emergency Management Agency (1997): NEHRP Guidelines for the Seismic Rehabilitation of Buildings. Report FEMA 273, Washington, DC.
- [3] Wang PH, Chang KC, Ou YC (2019): Capacity-Based Inelastic Displacement Spectra for Reinforced Concrete Bridge Columns. *Earthquake Engineering and Structural Dynamics*, 48(14): 1536-1555.
- [4] Wang PH, Ou YC, Chang KC (2017): A New Smooth Hysteretic Model for Ductile Flexural-dominated Reinforced Concrete Bridge Columns. *Earthquake Engineering and Structural Dynamics*, 46: 2237-2259.
- [5] American Association of State Highway and Transportation Officials (2011): Guide Specification for LRFD Seismic Bridge Design, LRFDSEIS-2, Washington, DC.
- [6] Park YJ, Ang AHS (1985): Mechanistic seismic damage model for reinforced concrete. *Journal of Structural Engineering (ASCE)*; 111(4):722–739.
- [7] Ministry of Transportation, and Communications (MOTC, 2019): Seismic bridge design specifications. Taipei, Taiwan (in Chinese).
- [8] Mahin SA, Bertero VV (1976): Problems in Establishing and Predicting Ductility in Aseismic Design. Proceedings of the International Symposium on Earthquake Structural Engineering: St. Louis, Missouri, US.